Clim. Past, 12, 241–253, 2016
www.clim-past.net/12/241/2016/
doi:10.5194/cp-12-241-2016

Climate of the Past
Open Access
EGU

Estimates of late middle Eocene pCO_2 based on stomatal density of modern and fossil *Nageia* leaves

X. Y. Liu, Q. Gao, M. Han, and J. H. Jin

State Key Laboratory of Biocontrol and Guangdong Provincial Key Laboratory of Plant Resources, School of Life Sciences, Sun Yat-sen University, Guangzhou 510275, China

Correspondence to: J. H. Jin (lssjjh@mail.sysu.edu.cn)

Received: 31 May 2015 – Published in Clim. Past Discuss.: 1 July 2015
Revised: 5 January 2016 – Accepted: 8 January 2016 – Published: 10 February 2016

Abstract. Atmospheric pCO_2 concentrations have been estimated for intervals of the Eocene using various models and proxy information. Here we reconstruct late middle Eocene (42.0–38.5 Ma) pCO_2 based on the fossil leaves of *Nageia maomingensis* Jin et Liu collected from the Maoming Basin, Guangdong Province, China. We first determine relationships between atmospheric pCO_2 concentrations, stomatal density (SD) and stomatal index (SI) using "modern" leaves of *N. motleyi* (Parl.) De Laub, the nearest living species to the Eocene fossils. This work indicates that the SD inversely responds to pCO_2, while SI has almost no relationship with pCO_2. Eocene pCO_2 concentrations can be reconstructed based on a regression approach and the stomatal ratio method by using the SD. The first approach gives a pCO_2 of 351.9 ± 6.6 ppmv, whereas the one based on stomatal ratio gives a pCO_2 of 537.5 ± 56.5 ppmv. Here, we explored the potential of *N. maomingensis* in pCO_2 reconstruction and obtained different results according to different methods, providing a new insight for the reconstruction of paleoclimate and paleoenvironment in conifers.

1 Introduction

The Eocene (55.8–33.9 Ma) generally was much warmer than present-day, although temperatures varied significantly across this time interval (Zachos et al., 2008). Climate of the early Eocene was extremely warm, particularly during the early Eocene Climatic Optimum (EECO; 51–53 Ma), and the Paleocene-Eocene Thermal Maximum (PETM; ∼ 55.9 Ma). However, global climatic conditions cooled significantly by the middle to late Eocene (40–36 Ma). Indeed, small, ephemeral ice-sheets and Arctic sea ice likely existed during the latest Eocene (Moran et al., 2006; Zachos et al., 2008).

Many authors have suggested that changes in temperature during the Phanerozoic were linked to atmospheric pCO_2 (Petit et al., 1999; Retallack, 2001; Royer, 2006). Central to these discussions are records across the Eocene, as this epoch spans the last major change from a "greenhouse" world to an "icehouse" world. The Eocene pCO_2 record remains incomplete and debated (Kürschner et al., 2001; Royer et al., 2001; Beerling et al., 2002; Greenwood et al., 2003; Royer, 2003). Most pCO_2 reconstructions have focused on the Cretaceous–Tertiary and Paleocene–Eocene boundaries (65–50 Ma) and the middle Eocene. In particular, there are few reconstructions for the late middle Eocene (Pagani et al., 2005; Maxbauer et al., 2014). In addition, the pCO_2 reconstruction results have varied based on different proxies. Various methods having been used in pCO_2 reconstruction mainly include the computer modeling methods: GEOCARB-I, GEOCARB-II, GEOCARB-III, GEOCARB-SULF and the proxies: ice cores, paleosol carbonate, phytoplankton, nahcolite, Boron, and stomata parameters.

The abundance of stomatal cells can be measured on modern leaves and well-preserved fossil leaves. Various plants show a negative correlation between atmospheric CO_2 concentration and stomatal density (SD), stomatal index (SI), or both. As such, these parameters have been determined in fossil leaves to reconstruct past pCO_2; examples include *Ginkgo* (Retallack, 2001, 2009a; Beerling et al., 2002; Royer, 2003; Kürschner et al., 2008; Smith et al., 2010), *Metasequoia* (Royer, 2003; Doria et al., 2011), *Taxodium* (Stults et al., 2011), *Betula* (Kürschner et al., 2001; Sun et al., 2012), *Neolitsea* (Greenwood et al., 2003), and *Quer-*

cus (Kürschner et al., 1996, 2001), *Laurus* and *Ocotea* (Kürschner et al., 2008). Recently, positive correlations between stomatal index or stomatal frequency and pCO_2 have been reported based on fossil *Typha* and *Quercus* (Bai et al., 2015; Hu et al., 2015). However, the tropical and subtropical moist broadleaf forest conifer tree *Nageia* has not been used previously in paleobotanical estimates of pCO_2 concentration.

Herein, we firstly document correlations between stomatal properties and atmospheric CO_2 concentrations using leaves of the extant species *Nageia motleyi* (Parl.) De Laub. that were collected over the last 2 centuries. This provides a training data set for application to fossil representatives of *Nageia*. We secondly measure stomatal parameters on fossil *Nageia* leaves from late middle Eocene of South China to estimate past CO_2 levels. The work provides further insights for discussing Eocene climate change.

2 Background

2.1 Stomatal proxy in pCO_2 research

Stomatal information gathered from careful examination of leaves has been widely used for reconstructions of past pCO_2 concentrations (Beerling and Kelly, 1997; Doria et al., 2011). The three main parameters are stomatal density (SD), which is expressed as the total number of stomata divided by area, epidermal density (ED), which is expressed as the total number of epidermal cells per area, and the stomatal index (SI), which is defined as the percentage of stomata among the total number of cells within an area [$SI = SD \times 100/(SD+ED)$]. Woodward (1987) considered that both SD and SI had inverse relationships with atmospheric CO_2 during the development of the leaves. Subsequently, McElwain (1998) created the stomatal ratio (SR) method to reconstruct pCO_2. SR is a ratio of the stomatal density or index of a fossil [$SD_{(f)}$ or $SI_{(f)}$] to that of corresponding nearest living equivalent [$SD_{(e)}$ or $SI_{(e)}$], expressed as follows:

$$SR = SI_{(e)}/SI_{(f)}. \quad (1)$$

The stomatal ratio method is a semi-quantitative method of reconstructing pCO_2 concentrations under certain standardizations. An example is the "Carboniferous standardization" (Chaloner and McElwain, 1997), where one stomatal ratio unit equals two RCO_2 units:

$$SR = 2RCO_2 \quad (2)$$

and the value of RCO_2 is the pCO_2 level divided by the pre-industrial atmospheric level (PIL) of 300 ppm (McElwain, 1998) or that of the year when the nearest living equivalent (NLE) was collected (Berner, 1994; McElwain, 1998):

$$RCO_2 = C_{(f)}/300 \text{ or } RCO_2 = C_{(f)}/C_{(e)}. \quad (3)$$

The estimated pCO_2 level can then be expressed as follows:

$$C_{(f)} = 0.5 \times C_{(e)} \times SD_{(e)}/SD_{(f)} \text{ or}$$
$$C_{(f)} = 0.5 \times C_{(e)} \times SI_{(e)}/SI_{(f)}, \quad (4)$$

where $C_{(f)}$ is the pCO_2 represented by the fossil leaf, and $C_{(e)}$ is the atmospheric CO_2 of the year when the leaf of the NLE species was collected (McElwain and Chaloner, 1995, 1996; McElwain 1998). The equation adapts to the pCO_2 concentration prior to Cenozoic.

Another standardization, the "Recent standardization" (McElwain, 1998), is expressed as one stomatal ratio unit being equal to one RCO_2 unit:

$$SR = 1RCO_2. \quad (5)$$

According to the equations stated above, the pCO_2 concentration can be expressed as

$$C_{(f)} = C_e \times SD_{(e)}/SD_{(f)} \text{ or } C_{(f)} = C_e \times SI_{(e)}/SI_{(f)}. \quad (6)$$

This standardization is usually used for reconstruction based on Cenozoic fossils (Chaloner and McElwain, 1997; McElwain, 1998; Beerling and Royer, 2002).

Kouwenberg et al. (2003) proposed some special stomatal quantification methods for conifer leaves with stomata arranged in rows. The stomatal number per length (SNL) is expressed as the number of abaxial stomata plus the number of adaxial stomata divided by leaf length in millimeters. Stomatal rows (SRO) are expressed as the number of stomatal rows in both stomatal bands. Stomatal density per length (SDL) is expressed as the equation $SDL = SD \times SRO$. True stomatal density per length (TSDL) is expressed as the equation TSDL = SD × band width (in millimeters). The band width on *Nageia motleyi* leaves was measured as leaf blade width.

2.2 Review of extant and fossil *Nageia*

The genus *Nageia*, including seven living species, is a special group of Podocarpaceae, a large family of conifers mainly distributed in the Southern Hemisphere. *Nageia* has broadly ovate-elliptic to oblong-lanceolate, multi-veined (without a mid-vein), spirally arranged or in decussate, and opposite or sub-opposite leaves (Cheng et al., 1978; Fu et al., 1999). Generally, *Nageia* is divided into two sections, *Nageia* Sect. *Nageia* and *Nageia* Sect. *Dammaroideae* (Mill 1999, 2001). Both sections are mainly distributed in southeast Asia and Australasia from north latitude 30° to nearly the equator (Fu, 1992; Fig. 1). Four species of the *N.* section *Nageia* – *Nageia nagi* (Thunberg) O. Kuntze, *N. fleuryi* (Hickel) De Laub., *N. formosensis* (Dummer) C. N. Page, and *N. nankoensis* (Hayata) R. R. Mill – have hypostomatic leaves where stomata only occur on the abaxial side. One species of this section – *N. maxima* (De Laub.) De Laub. – is characterized by amphistomatic leaves, but where only a few stomata are found

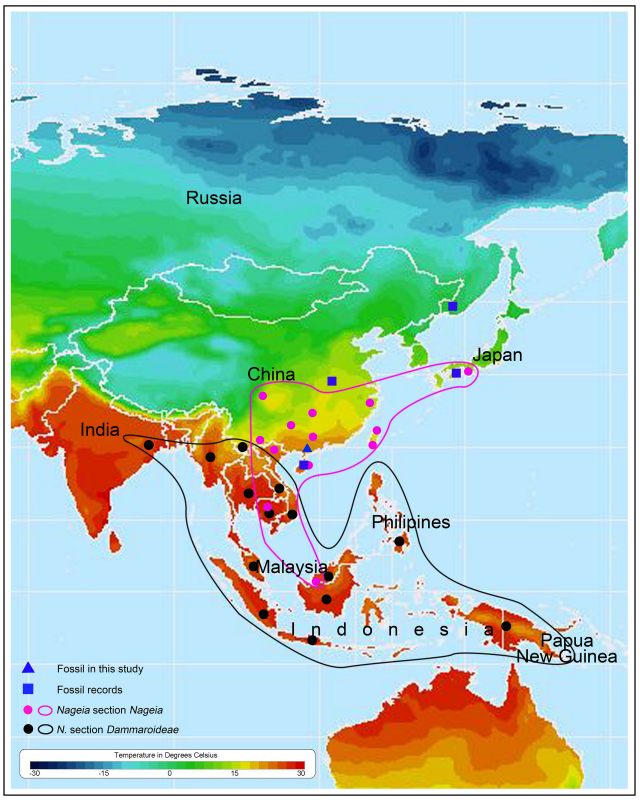

Figure 1. Map showing the distribution of extant and fossil *Nageia* and their mean annual temperature (modified after the map from http://nelson.wisc.edu/sage/data-and-models/atlas/maps/avganntemp/atl_avganntemp.jpg).

on the adaxial side (Hill and Pole, 1992; Sun, 2008). Both *N. wallichiana* (Presl) O. Kuntze and *N. motleyi* of the *N.* section *Dammaroideae* are amphistomatic with abundant stomata distributed on both sides of the leaf. This is especially true for *N. motleyi*, which has approximately equal stomata numbers on both surfaces (Hill and Pole, 1992; Sun, 2008).

The fossil record of *Nageia* can be traced back to the Cretaceous. Krassilov (1965) described *Podocarpus* (*Nageia*) *sujfunensis* Krassilov from the Lower Cretaceous of Far East Russia. Kimura et al. (1988) reported *Podocarpus* (*Nageia*) *ryosekiensis* Kimura, Ohanaet Mimoto, an ultimate leafy branch bearing a seed, from the Early Barremian in southwestern Japan. In China, a Cretaceous petrified wood, *Podocarpus* (*Nageia*) *nagi* Pilger, was discovered from the Dabie Mountains in central Henan, China (Yang et al., 1990). Jin et al. (2010) reported an upper Eocene *Nageia* leaf named *N. hainanensis* Jin, Qiu, Zhu et Kodrul from the Changchang Basin of Hainan Island, South China. Recently, Liu et al. (2015) found another leaf species *N. maomingensis* Jin et Liu from upper middle Eocene of Maoming Basin, South China. Although some of the *Nageia* fossil materials described in the above studies (Krassilov, 1965; Jin et al., 2010; Liu et al., 2015) have well-preserved cuticles, these studies are mainly concentrated on morphology, systematics, and phytogeography.

Here we try to reconstruct the pCO_2 concentration based on stomatal data of *Nageia maomingensis* Jin et Liu. Among the modern *Nageia* species mentioned above, *N. motleyi* was considered as the NLE species of *N. maomingensis* (Liu et al., 2015). However, because of the species-specific inverse relationship between atmospheric CO_2 partial pressure and SD (Woodward and Bazzaz, 1988), it is necessary to explore whether the SD and SI of *N. motleyi* show negative correlations with the CO_2 concentration before applying the stomatal method. Both *N. maomingensis* and *N. motleyi* are amphistomatic, suggesting that both upper and lower surfaces of leaves might be used to estimate the pCO_2 concentrations.

3 Material and methods

3.1 Extant leaf preparation

We examined 12 specimens of extant *Nageia motleyi* from different herbaria (Table 1). We removed one or two leaves from each specimen, and took three fragments (0.25 mm^2) from every leaf (Fig. 2a) and numbered them for analysis.

The numbered fragments were boiled for 5–10 min in water. Subsequently, after being macerated in a mixed solution of 10 % acetic acid and 10 % H_2O_2 (1 : 1) and heated in the thermostatic water bath at 85 °C for 8.5 h, the reaction was stopped when the specimen fragments turned white and semitransparent. The cuticles were then rinsed with distilled water until the pH of the water became neutral. After, the cuticles were treated in Schulze's solution (one part of potassium chlorate saturated solution and three part of concentrated nitric acid) for 30 min, rinsed in water, and then treated with 8 % KOH (up to 30 min). The abaxial and adaxial cuticles were separated with a hair mounted on needle. Finally, the cuticles were stained with 1 % Safranin T alcoholic solution for 5 min, sealed with Neutral Balsam and observed under LM.

3.2 Fossil leaf preparation

Maoming Basin (21°42′33.2″ N, 110°53′19.4″ E) is located in southwestern Guangdong, South China including Cretaceous and Tertiary strata. Tertiary strata are fluvial and lacustrine sedimentary units, divided into the Gaopengling, Laohuling, Shangcun, Huangniuling and Youganwo formations in descending order, aged from late Eocene to early Oligocene (Wang et al., 1994).

Four fossil leaves of *Nageia maomingensis* were recovered from the Youganwo (MMJ1-001) and Huangniuling (MMJ2-003, MMJ2-004 and MMJ3-003) formations of Maoming Basin, South China. Further information on the sections is provided by Liu et al. (2015). Importantly, the formations span a depositional age of approximately 42.0–38.5 Ma which was considered as late Eocene by Wang et al. (1994),

Table 1. Modern *Nageia motleyi* (Parl.) De Laub. samples and atmospheric CO_2 values of their collection dates from ice core data (Brown, 2010).

Herbarium	Collection number	Collecting locality	Collectors	Number of leaf samples	Collection date	CO_2 (ppmv)
LE	No. 2649	Malaysia	O. Beccari,	1	1868	289.23
A/GH	No. bb. 17229	150 m, Riau on Ond. Karimon	Neth. Ind. For. Service	2	1932	306.19
A/GH	No. bb. 18328	5 m, Z. O. afd. v. Borneo Tidoengsche Landen	Neth. Ind. For. Service	2	1934	306.46
A/GH	No. bb. 21151	500 m, Z. O. afd. Borneo, Poeroek Tjahoe Tahoedjan	Neth. Ind. For. Service	2	1936	306.76
KEP	No. 30887	Kata Tinggi, Johor, Malaysia	E. J. H. Corner	1	1936	306.76
KEP	No. 57329	Batang Padang, Perak, Malaysia	Unkonwn	2	1947	309.82
KEP	No. 57330	Batang Padang, Perak, Malaysia	Unkonwn	2	1947	309.82
KEP	No. 55897	Batang Padang, Perak, Malaysia	Unkonwn	2	1947	309.82
KEP	No. 61064	Batang Padang, Perak, Malaysia	Syed Woh	2	1947	309.82
E	No. bb. 40798	51 m, Kuala Trengganu-Besut Road, Bukit Bintang Block, Gunong Tebu Forest reserve, Malaysia	J. Sinclair and K. bin Salleh	2	1955	313.73
KEP	No. 80548	Gombak, Selangor, Malaysia	Rahim	1	1965	320.04
KEP	No. 33343	Jelebu, Negeri Sembilan, Malaysia	S. K. Yap	2	1987	348.98

Note: A/GH: Harvard University Herbarium, Harvard University, 22 Divinity Avenue, Cambridge, Massachusetts 02138, USA (www.huh.harvard.edu).
E: The Herbarium of Royal Botanic Garden, Edinburgh EH3 5LR, Scotland, UK (www.rbge.org.uk).
LE: The Herbarium of the V. L. Komarov Botanical Institute of the Russian Academy of Sciences, Prof. Popov Street 2, Saint Petersburg 197376, Russia (www.binran.ru).
KEP: Kepong Herbarium, Forest Research Institute Malaysia, 52109 Kepong, Selangor, Malaysia (http://www.frim.gov.my/).

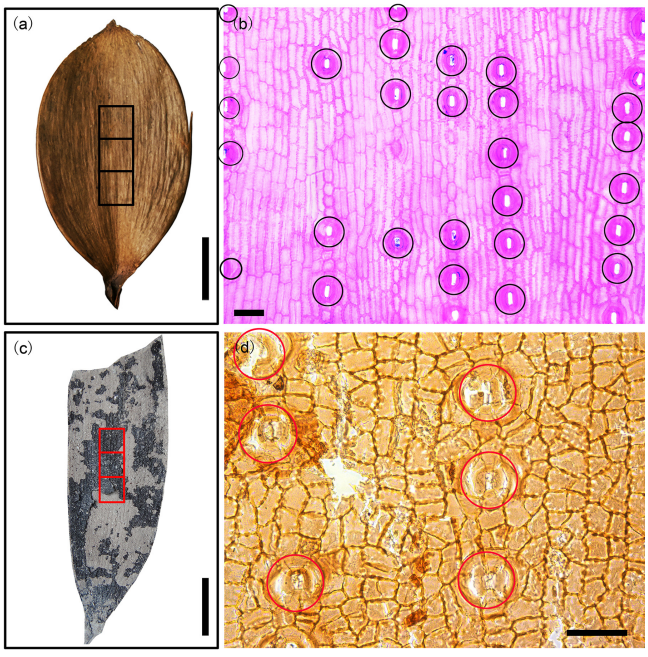

Figure 2. Sampling areas and counting rules are shown. **(a)** *Nageia motleyi* (Parl.) De Laub. leaf. Black squares in the middle of the leaf show the sampling areas for preparing the cuticles. **(b)** The abaxial side of the cuticle from *N. motleyi* leaf. Black circles show the counted stomatal complexes. **(c)** *N. maomingensis* Jin et Liu. Red squares in the middle of the leaf indicate the sampling areas. **(d)** The abaxial side of the fossil cuticle. Red circles show the counted stomatal complexes. Scale bars: **(a)** and **(c)** = 1 cm; **(b)** and **(d)** = 50 µm.

but it can be recognized as late middle Eocene according to Walker and Geissman (2009).

Macrofossil cuticular fragments were taken from the middle part of each fossil leaf (Fig. 2c) and directly treated with Schulze's solution for approximately 1 h and 5–10% KOH for 30 min (Ye, 1981). The cuticles were observed and photographed under a Carl Zeiss Axio Scope A1 light microscope (LM). All fossil specimens and cuticle slides are housed in the Museum of Biology of Sun Yat-sen University, Guangzhou, China.

3.3 Stomatal counting strategy and calculation methods

The basic stomatal parameters, SD, ED, and SI were counted based on analyzing pictures taken with a light microscope (LM). A total of 2816 pictures (200× magnification of Zeiss LM) of cuticles from 21 leaves of *N. motleyi* were counted. Each counting field was 0.366 mm^2. We used a standard sampling protocol (Poole and Kürschner, 1999), counting all full stomata in the image plus stomata straddling the left and top margins, as presented in Fig. 2b and d.

The SNL, SRO, SDL, and TSDL were also determined based on LM images. A total of 2293 pictures (200× magnification of Zeiss LM) of the cuticles from 21 leaves of *N. motleyi* were counted. Each counting field was 0.366 mm^2. None of the aforementioned counting areas overlapped and they were larger than the minimum area (0.03 mm^2) for statistics (Poole and Kürschner, 1999). In this study, the stomatal data of both surfaces are applied in pCO_2 reconstruction because both the fossil and NLE species are amphistomatic.

4 Results

4.1 Correlations between the CO_2 concentrations and stomatal parameters of *Nageia motleyi*

The SD and SI data of the adaxial sides of *N. motleyi* leaves are presented in Table 2. The SDs and SIs average 62.28 mm^{-2} and 3.30 %, respectively. However, the SDs and SIs data of the abaxial sides, summarized in Table 3, give higher average values (70.03 mm^{-2} in SDs and 3.90 % in SIs) than those from the adaxial sides. The combined SD and

Table 2. Summary of stomatal parameters of the adaxial surface from modern *Nageia motleyi* (Parl.) De Laub.

Collection number	Collection date	CO_2 (ppmv)	SD (mm^{-2})					SI (%)				
			x	σ	s.e.	t^*s.e.	n	x	σ	s.e.	t^*s.e.	n
No. 2649	1868	289.23	78.60	15.44	1.41	2.76	120	3.44	0.66	0.06	0.12	120
No. bb. 17229	1932	306.19	62.14	17.20	1.78	3.50	93	2.89	0.68	0.07	0.14	93
No. bb. 18328	1934	306.46	64.57	15.05	1.58	3.11	90	3.39	1.01	0.11	0.21	90
No. bb. 21151	1936	306.76	65.45	11.14	1.17	2.30	90	3.94	0.74	0.08	0.15	90
No. SFN30887	1936	306.76	66.90	16.10	1.27	2.49	161	3.61	0.92	0.07	0.14	161
No. 61064	1947	309.82	56.71	16.81	1.95	3.83	74	3.27	1.26	0.15	0.29	74
No. 57330	1947	309.82	67.37	15.97	2.04	4.01	61	3.70	0.82	0.10	0.20	61
No. 57329	1947	309.82	67.85	15.61	1.70	3.34	84	3.50	0.90	0.10	0.20	84
No. 55897	1947	309.82	66.74	14.10	1.78	3.48	63	3.18	0.66	0.08	0.16	63
No. 40798	1955	313.73	45.89	13.81	1.12	2.20	151	3.03	0.87	0.07	0.14	151
No. KEP80548	1965	320.04	52.94	11.25	0.85	1.67	175	2.81	0.61	0.05	0.09	175
No. FRI33343	1987	348.98	52.25	12.05	0.77	1.51	242	2.87	0.69	0.04	0.09	242
Mean	–	–	62.28	14.54	1.45	2.85	117	3.30	0.52	0.08	0.16	117

Note: x: mean, σ: standard deviation, s.e.: standard error of mean, n: numbers of photos counts (200×), t^*s.e.: 95 % confidence interval.

Table 3. Summary of stomatal parameters of the abaxial surface from modern *Nageia motleyi* (Parl.) De Laub.

Collection number	Collection date	CO_2 (ppmv)	SD (mm^{-2})					SI (%)				
			x	σ	s.e.	t^*s.e.	n	x	σ	s.e.	t^*s.e.	n
No. 2649	1868	289.23	82.71	12.23	1.02	2.00	144	3.89	0.58	0.05	0.09	144
No. bb. 17229	1932	306.19	69.16	14.23	1.48	2.90	93	3.13	0.58	0.06	0.12	93
No. bb. 18328	1934	306.46	69.92	14.38	1.52	2.97	90	3.99	1.08	0.11	0.22	90
No. bb. 21151	1936	306.76	75.68	15.74	1.66	3.25	90	4.66	0.88	0.09	0.18	90
No. SFN30887	1936	306.76	76.18	12.51	0.99	1.93	161	4.42	0.89	0.07	0.14	161
No. 61064	1947	309.82	60.93	11.02	1.39	2.72	63	3.05	0.62	0.08	0.15	63
No. 57330	1947	309.82	75.82	14.14	1.82	3.58	60	4.38	0.84	0.11	0.21	60
No. 57329	1947	309.82	71.74	16.84	1.75	3.42	93	3.72	0.62	0.06	0.13	93
No. 55897	1947	309.82	78.63	13.41	1.75	3.42	59	4.41	1.00	0.13	0.26	59
No. 40798	1955	313.73	53.22	13.88	1.12	2.19	155	3.71	0.93	0.07	0.15	155
No. KEP80548	1965	320.04	67.22	13.97	1.07	2.09	171	3.70	0.80	0.06	0.12	171
No. FRI33343	1987	348.98	59.09	12.10	0.79	1.55	233	3.69	0.86	0.06	0.11	233
Mean	–	–	70.03	13.70	1.36	2.67	118	3.90	0.81	0.08	0.16	118

Note: x: mean, σ: standard deviation, s.e.: standard error of mean, n: numbers of photos counts (200×), t^*s.e.: 95 % confidence interval.

SI of the adaxial and abaxial surfaces average 66.14 mm^{-2} and 3.60 %, respectively (Table 4).

Figure 3 shows the relationships between the stomatal parameters (SD and SI) of modern *N. motleyi* and the atmospheric CO_2 concentration (SD-CO_2 relationship and SI-CO_2 relationship). R^2 values in the SD-CO_2 relationship from the adaxial and abaxial surfaces of *N. motleyi* are up to 0.4667 and 0.3824 (Fig. 3a, b), suggesting that the stomatal densities of *N. motleyi* are inverse to the CO_2 concentrations. However, Fig. 3c and d indicate no relationship between the SIs and CO_2 concentrations for the extremely low level of the R^2 values (0.2558 and 0.0248). Figure 3e and f based on the combined data also show that SD inversely responds to the atmospheric CO_2 concentration ($R^2 = 0.4421$), while SI has almost no relationship with the atmospheric CO_2 concentration ($R^2 = 0.1177$).

The mean values of SNL, SDL, and TSDL are 9.81, 326.39 and 1226.93 no. mm^{-1}, respectively (Table 5). Figure 4 shows the relationships between SNL (SDL, TSDL) and CO_2 concentrations. The low R^2 values in Fig. 4a and c indicate that SNL ($R^2 = 0.0643$) and TSDL ($R^2 = 0.0788$) have no relationship with the CO_2 concentration in this study. Figure 4b shows that there is a weak reverse relevance between SDL and the CO_2 concentration ($R^2 = 0.3154$).

Compared with the SDL method, the SD-based method shows a larger R^2 value, indicating a stronger relevance between the SD and CO_2 concentrations. In this study, the pCO_2 is reconstructed based on the regression equations of SD-CO_2 relationship. Additionally, the stomatal ratio

Table 4. Summary of stomatal parameters of the combined data of the adaxial and abaxial surfaces from modern *Nageia motleyi* (Parl.) De Laub.

Collection number	Collection date	CO_2 (ppmv)	SD (mm^{-2})					SI (%)				
			x	σ	s.e.	t^*s.e.	n	x	σ	s.e.	t^*s.e.	n
No. 2649	1868	289.23	80.84	13.74	0.85	1.66	264	3.69	0.66	0.04	0.08	264
No. bb. 17229	1932	306.19	65.65	16.13	1.18	2.32	186	3.01	0.64	0.05	0.09	186
No. bb. 18328	1934	306.46	67.24	14.92	1.11	2.18	180	3.69	1.08	0.08	0.16	180
No. bb. 21151	1936	306.76	70.57	14.53	1.08	2.12	180	4.30	0.89	0.07	0.13	180
No. SFN30887	1936	306.76	71.54	15.12	0.84	1.65	322	4.01	0.99	0.05	0.11	322
No. 61064	1947	309.82	58.65	14.54	1.24	2.43	137	3.17	1.02	0.09	0.17	137
No. 57330	1947	309.82	71.56	15.61	1.42	2.78	121	4.03	0.89	0.08	0.16	121
No. 57329	1947	309.82	69.90	16.33	1.23	2.41	177	3.62	0.77	0.06	0.11	177
No. 55897	1947	309.82	72.49	14.95	1.35	2.65	122	3.77	1.04	0.09	0.18	122
No. 40798	1955	313.73	49.60	14.31	0.82	1.60	306	3.37	0.96	0.05	0.11	306
No. KEP80548	1965	320.04	60.00	14.53	0.78	1.53	346	3.25	0.84	0.05	0.09	346
No. FRI33343	1987	348.98	55.61	12.53	0.58	1.13	475	3.28	0.88	0.04	0.08	475
Mean	–	–	66.14	14.77	1.04	2.08	235	3.60	0.89	0.06	0.12	235

Note: x: mean, σ: standard deviation, s.e.: standard error of mean, n: numbers of photos counts (200×), t^*s.e.: 95 % confidence interval.

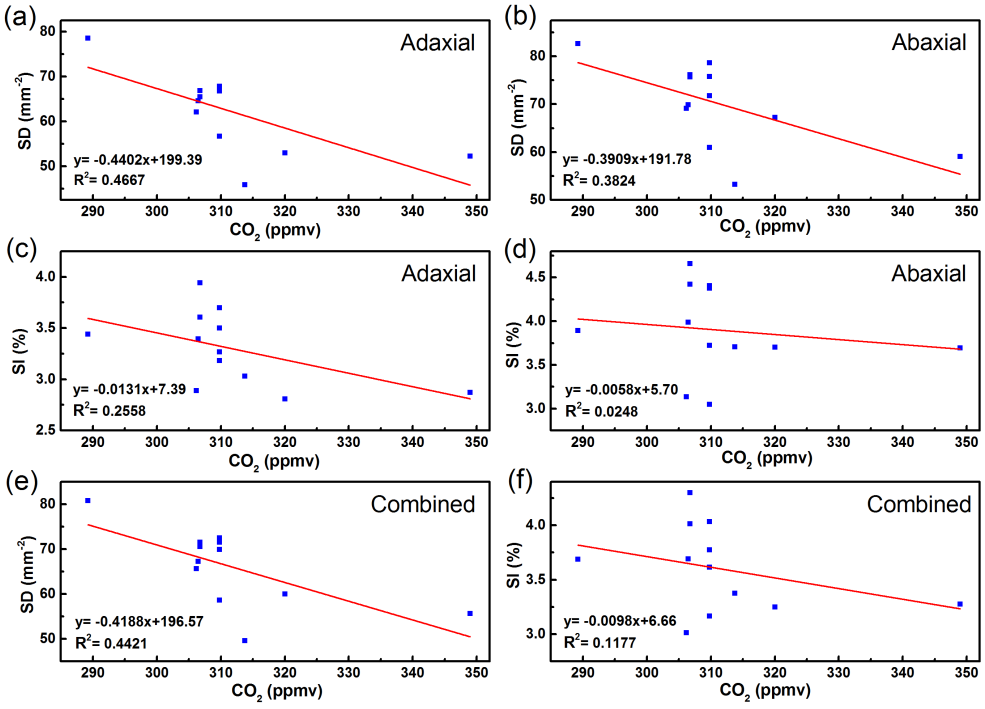

Figure 3. Correlation between SD and SI versus CO_2 concentration for modern *Nageia motleyi*. **(a)** Trends of SD with CO_2 concentration for the adaxial surface. **(b)** Trends of SD with CO_2 concentration for the abaxial surface. **(c)** Trends of SI with CO_2 concentration for the adaxial surface. **(d)** Trends of SI with CO_2 concentration for the abaxial surface. **(e)** Trends of SD with CO_2 concentration for the combined data of both leaf surfaces. **(f)** Trends of SI with CO_2 concentration for the combined data of both leaf surfaces.

method can be also used in estimating pCO_2 concentration of late middle Eocene based on stomatal densities (SDs) of the fossil species *N. maomingensis* and extant species *N. motleyi*. The SD results of specimen No. 18328 are selected to reconstruct the pCO_2 concentration, because they are closest to the fitted equations in Fig. 3. This specimen was collected by the Netherlands Indies Forest Service from Borneo Tidoengsche Landen, in 1934 at an altitude of 5 m and CO_2 concentration of 306.46 ppmv (Brown, 2010).

Table 5. Summary of stomatal parameters from modern *Nageia motleyi* (Parl.) De Laub. (Kouwenberg et al., 2003).

Collection number	Collection date	CO_2 (ppmv)	SNL	SDL	TSDL	*n*
No. 2649	1868	289.23	11.64	394.38	1455.10	264
No. bb. 17229	1932	306.19	9.19	337.98	1280.12	186
No. bb. 18328	1934	306.46	8.71	378.92	1277.63	180
No. bb. 21151	1936	306.76	9.62	376.93	1517.21	180
No. SFN30887	1936	306.76	10.55	325.08	735.38	240
No. 61064	1947	309.82	8.19	282.04	1200.66	133
No. 57330	1947	309.82	9.67	397.83	1397.33	119
No. 57329	1947	309.82	10.13	350.98	1672.50	176
No. 55897	1947	309.82	10.48	379.06	1486.13	122
No. 40798	1955	313.73	10.29	175.14	933.85	305
No. KEP80548	1965	320.04	9.36	266.16	585.72	263
No. FRI33343	1987	348.98	9.84	252.20	1181.51	125
Mean	–	–	9.81	326.39	1226.93	191

4.2 The pCO_2 estimates results

4.2.1 The regression approach

The summary of stomatal parameters of the fossil *Nageia* and reconstruction results are provided in Tables 6–8. The mean SD and SI values of the adaxial surface are 44.5 mm^{-2} and 1.8 %, respectively (Table 6). The mean SD and SI values of the abaxial surface are 48.9 mm^{-2} and 2.07 %, respectively (Table 7).

Based on the regression approach, the pCO_2 was reconstructed as 351.9 ± 6.6 ppmv and 365.6 ± 7.7 ppmv according to the SD of adaxial and abaxial sides. The combined SD value is an average of 46.6 mm^{-2} (Table 8), giving the reconstructed pCO_2 of 358.1 ± 5.0 ppmv.

4.2.2 The stomatal ratio method

Mean SR value of the adaxial side ($SR = 1.75 \pm 0.18$) is a little larger than that of the abaxial side ($SR = 1.62 \pm 0.12$) in fossil *Nageia* leaves (Tables 6, 7). The pCO_2 reconstruction results are 537.5 ± 56.5 ppmv (Table 6) and 496.1 ± 35.7 ppmv (Table 7) based on the adaxial and abaxial cuticles, respectively. Based on the combined SD of both leaf sides, the pCO_2 result is 519.9 ± 35.0 ppmv.

The partial pressure of CO_2 decreases with elevation (Gale, 1972). Jones (1992) proposed that the relationship between elevation and partial pressure in the lower atmosphere can be expressed as $P = -10.6E + 100$, where E is elevation in kilometers and P is the percentage of partial pressure relative to sea level. Various studies corroborate that SI and SD of many plants have positive correlations with altitude (Körner and Cochrane, 1985; Woodward, 1986; Woodward and Bazzaz, 1988; Beerling et al., 1992; Rundgren and Beerling, 1999) while they are negatively related to the partial pressure of CO_2 (Woodward and Bazzaz, 1988). Therefore, it is essential to take elevation calibration into account during pCO_2 concentration estimates. However, Royer (2003) pointed out that it is unnecessary to provide this conversion

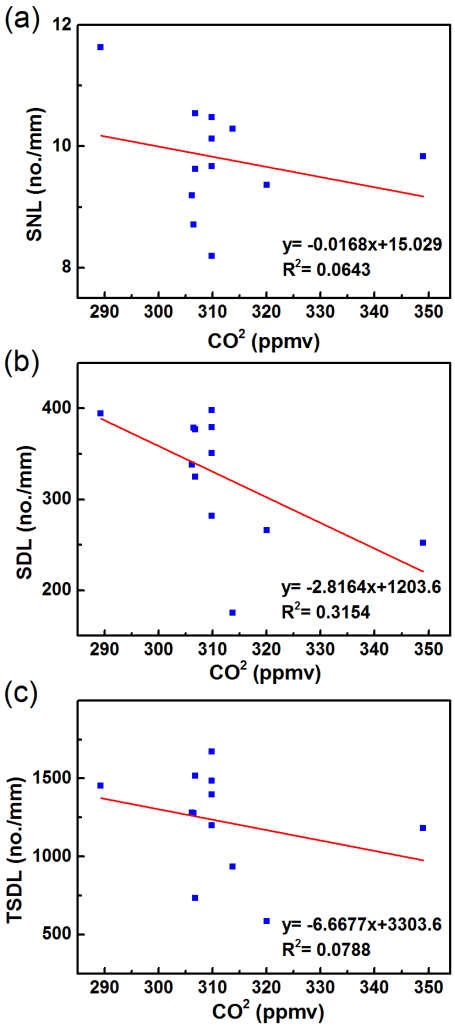

Figure 4. Correlation between SNL, SDL, and TSDL versus CO_2 concentration for modern *Nageia motleyi*. **(a)** Trends of SNL with CO_2 concentration for the adaxial surface. **(b)** Trends of SDL with CO_2 concentration for the adaxial surface. **(c)** Trends of TSDL with CO_2 concentration for the adaxial surface.

when trees lived at < 250 m in elevation. In this paper, the nearest living equivalent species, *Nageia motleyi*, grows at 5 m in elevation with $P = 99.9$, suggesting that CO_2 concentration estimates were only underestimated by 0.1 %. Consequently, no correction is needed for the reconstruction result in this study. After being projected into a long-term carbon cycle model (GEOCARB III; Berner and Kothavalá, 2001), the results of this study compare well with CO_2 concentrations for corresponding age within their error ranges (Fig. 5).

Table 6. Summary of stomatal parameters of the adaxial surface of fossil *Nageia* and pCO_2 [$C_{(f)}$] estimates results.

Species	Age	SD (mm^{-2})				SI (%)				SR		pCO_2 (ppmv)		$C_{(f)}$ (ppmv)	
		x	σ	s.e.	n	x	σ	s.e.	n	x	t^*s.e.	x	t^*s.e.	x	t^*s.e.
MMJ1-001	Late Eocene	52.5	17.1	3.1	30	2.08	0.7	0.1	30	1.40	0.20	333.6	13.9	428.7	62.0
MMJ2-003	Late Eocene	42.3	12.9	2.4	30	1.80	0.6	0.1	30	1.82	0.41	356.8	10.5	557.6	126.2
MMJ2-004	Late Eocene	39.9	13.6	2.5	30	1.66	0.6	0.1	30	1.88	0.33	362.4	11.0	576.5	101.9
MMJ3-003a	Late Eocene	43.2	17.7	3.2	30	1.67	0.7	0.1	30	1.92	0.44	354.8	14.4	587.2	135.7
Mean	Late Eocene	44.5	16.3	1.5	120	1.80	0.7	0.1	120	1.75	0.18	351.9	6.6	537.5	56.5

Note: x: mean, σ: standard deviation, s.e.: standard error of mean, n: numbers of photos counts (400×), t^*s.e.: 95 % confidence interval, pCO_2: the result based the regression approach, $C_{(f)}$: the result based on the stomatal method.

Table 7. Summary of stomatal parameters of the abaxial surface of fossil *Nageia* and pCO_2 [$C_{(f)}$] estimates results.

Species	Age	SD (mm^{-2})				SI (%)				SR		pCO_2 (ppmv)		$C_{(f)}$ (ppmv)	
		x	σ	s.e.	n	x	σ	s.e.	n	x	t^*s.e.	x	t^*s.e.	x	t^*s.e.
MMJ1-001	Late Eocene	47.7	17.7	3.2	30	2.11	0.8	0.2	30	1.68	0.24	368.6	16.2	515.6	72.3
MMJ2-003	Late Eocene	50.9	18.3	3.3	30	2.12	0.8	0.1	30	1.59	0.23	360.9	16.6	486.0	70.7
MMJ2-004	Late Eocene	48.2	15.8	2.9	30	2.14	0.7	0.1	30	1.65	0.25	367.4	14.5	504.6	77.3
MMJ3-003a	Late Eocene	48.9	12.6	2.7	22	1.85	0.5	0.1	22	1.54	0.19	365.4	13.5	472.3	59.0
Mean	Late Eocene	48.9	16.2	1.5	112	2.07	0.7	0.1	112	1.62	0.12	365.6	7.7	496.1	35.7

Note: x: mean, σ: standard deviation, s.e.: standard error of mean, n: numbers of photos counts (400×), t^*s.e.: 95 % confidence interval, pCO_2: the result based the regression approach, $C_{(f)}$: the result based on the stomatal method.

Table 8. Summary of stomatal parameters of the combined data of the adaxial and abaxial surfaces of fossil *Nageia* and pCO_2 [$C_{(f)}$] estimates results.

Species	Age	SD (mm^{-2})				SI (%)				SR		pCO_2 (ppmv)		$C_{(f)}$ (ppmv)	
		x	σ	s.e.	n	x	σ	s.e.	n	x	t^*s.e.	x	t^*s.e.	x	t^*s.e.
MMJ1-001	Late Eocene	50.1	17.5	2.3	60	2.09	0.8	0.1	60	1.54	0.16	349.7	10.6	471.2	47.8
MMJ2-003	Late Eocene	46.5	16.3	2.1	60	1.96	0.7	0.1	60	1.71	0.25	358.3	9.8	524.1	75.7
MMJ2-004	Late Eocene	44.0	15.8	2.0	60	1.90	0.7	0.1	60	1.77	0.17	364.3	9.5	542.9	52.6
MMJ3-003a	Late Eocene	45.6	16.1	2.2	52	1.75	0.6	0.1	52	1.78	0.29	360.4	10.4	544.6	88.3
Mean	Late Eocene	46.6	16.4	1.1	232	1.93	0.7	0.1	232	1.70	0.11	358.1	5.0	519.9	35.0

Note: x: mean, σ: standard deviation; s.e.: standard error of mean; n: numbers of photos counts (400×); t^*s.e.: 95 % confidence interval. pCO_2: the result based the regression approach; $C_{(f)}$: the result based on the stomatal method.

5 Discussion

5.1 Stomatal parameters response to CO_2

For modern *Nageia*, we find that SD decreases as atmospheric CO_2 concentrations increase, but that SI does not. Generally, SI is more sensitive in response to the atmospheric CO_2 concentration than SD (Beerling, 1999; Royer, 2001). However, the reverse case has been observed from some flora. For example, Kouwenberg et al. (2003) reported that SD is better than SI in reflecting the negative relationships with CO_2 in conifer needles, accounting for the special paralleled mode of the ordinary epidermal and stomatal formation. Although *Nageia* is broad-leaved rather than needle-leaved, it also has well-paralleled epidermal cells.

Compared with SD, the SDL has weaker correlation with CO_2 at a smaller R^2. The SNL and TSDL have no response to the change of CO_2. The insensitivity of SNL, SDL, and TSDL might account for the characters of broad-leaved leaf shape and paralleled epidermal cells. The SNL should be applied to conifer needles with single file of stomata (Kouwenberg et al., 2003). The SDL and TSDL were considered as the most appropriate method when the stomatal rows grouped in bands in a hypo- or amphistomatal conifer needle species (Kouwenberg et al., 2003). Considering all the stomatal parameters above, SD appears to be the most sensitive to CO_2.

The SD-CO_2 correlation shows one value from leaf No. 40798 offset from the others. The SI-CO_2 correlation shows different offset values in different leaf sides. The offset values might be affected by leaf maturity and light intensity. However, it is hard to distinguish whether a fossil leaf was young or mature, or grew in a sunny or shady environment.

The R^2 value (0.5) of SD-CO_2 based on the adaxial side is higher than from the abaxial side and the combination of both sides, indicating that the correlation of SD-CO_2 is stronger than the other parameters herein. Therefore, the SD on the adaxial side is the best in reconstructing pCO_2. The

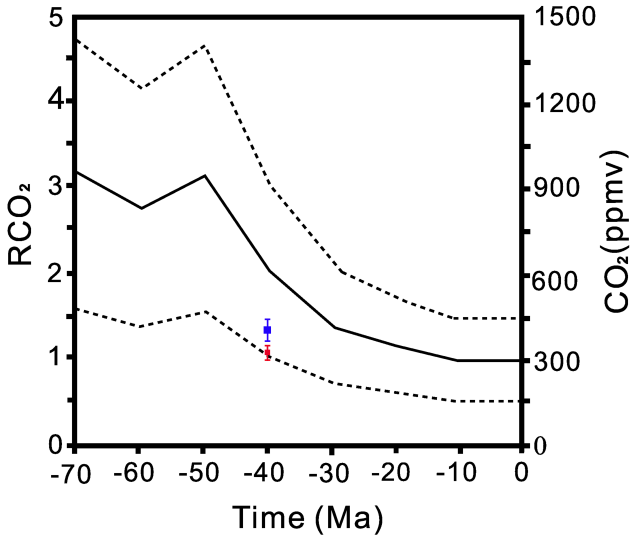

Figure 5. The pCO_2 reconstruction results and extant CO_2 concentrations are projected onto the long-term carbon cycle model (GEOCARB III; Berner and Kothavalá, 2001). The pCO_2 results based on the regression approach and stomatal ratio method are represented by red and blue squares, respectively.

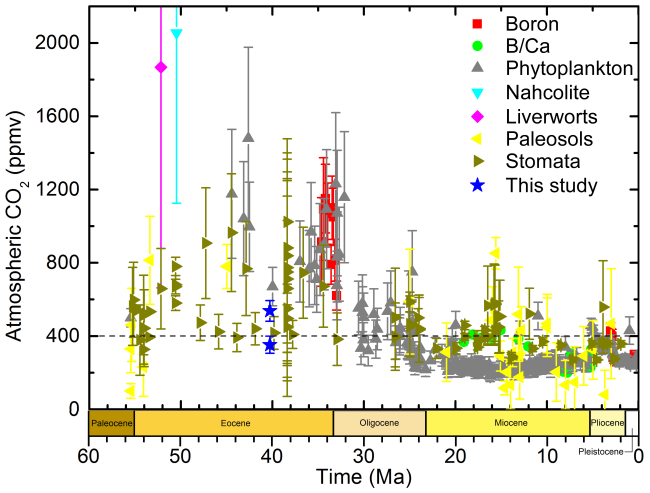

Figure 6. Atmospheric CO_2 estimates from proxies over the past 60 million years. The horizontal dashed line indicates monthly atmospheric CO_2 concentration for March 2015 at Mauna Loa, Hawaii (401.5 ppmv) (Pieter and Keeling, 2015). The vertical lines show the error bars. The data are from the supporting data of Beerling and Royer (2011) and references in Table 9. The lower blue star shows the reconstructed result based on the regression approach. The higher one presents the result of stomatal ratio method.

reconstruction result based on the regression approach is 351.9±6.6 ppmv lower than the one based on the stomatal ratio method (Table 6), and it is relatively lower than the results based on the other proxies (Fig. 6; Freeman and Hayes, 1992; Pagani et al., 2005; Maxbauer et al., 2014). However, the result based on stomatal ratio method is 537.5 ± 56.5 ppmv, which is fairly close to GEOCARB III predictions (Fig. 5) and historical reconstruction trends (Fig. 6).

5.2 Paleoclimate reconstructed history

The pCO_2 levels throughout the Cenozoic were generally lower than during much of the Cretaceous, but probably also decreased significantly from the early to late Eocene. However, there is a wide range of estimates for the Eocene (Koch et al., 1992; Sinha and Stott, 1994; Ekart et al., 1999; Greenwood et al., 2003; Royer, 2003; Pagani et al., 2005; Wing et al., 2005; Lowenstein and Demicco, 2006; Fletcher et al., 2008; Zachos et al., 2008; Beerling et al., 2009; Bijl et al., 2010; Smith et al., 2010; Doria et al., 2011; Kato et al., 2011; Maxbauer et al., 2014).

Smith et al. (2010) reconstructed the value of the early Eocene pCO_2 ranging from 580 ± 40 to 780 ± 50 ppmv using the stomatal ratio method (recent standardization) based on both SI and SD. A climatic optimum occurred in the middle Eocene (MECO): the reconstructed CO_2 concentrations are mainly between 700 and 1000 ppmv during the late middle Eocene climate transition (42–38 Ma) using stomatal indices of fossil *Metasequoia* needles, but concentrations declined to 450 ppmv toward the top of the investigated section (Doria et al., 2011). Jacques et al. (2014) used CLAMP

Table 9. pCO_2 estimates proxies and corresponding references.

Proxies	References
Boron	Pearson et al. (2009), Seki et al. (2010)
B / Ca	Tripati et al. (2009)
Phytoplankton	Freeman and Hayes (1992), Stott (1992), Pagani et al. (1999, 2005), Henderiks and Pagani (2008), Seki et al. (2010)
Nahcolite	Lowenstein and Demicco (2006)
Liverworts	Fletcher et al. (2008)
Paleosols	Cerling (1992), Koch et al. (1992), Ekart et al. (1999), Royer et al. (2001), Nordt et al. (2002), Retallack (2009b), Huang et al. (2013)
Stomata	Van der Burgh et al. (1993), Kürschner et al. (1996, 2001, 2008), McElwain (1998), Royer et al. (2001, 2003), Greenwood et al. (2003), Beerling et al. (2009), Retallack (2009a), Smith et al. (2010), Doria et al. (2011), Roth-Nebelsick et al. (2012; 2014), Grein et al. (2013), Maxbauer et al. (2014)

to calibrate climate change in Antarctica during the early-middle Eocene, suggesting a seasonal alternation of high- and low-pressure systems over Antarctica during the early-middle Eocene. Spicer et al. (2014) also reconstructed a relatively lower cool temperature than $\delta^{18}O$ records (Keating-

Bitonti et al., 2011) in the middle Eocene of Hainan Island, South China using CLAMP, indicating a not uniformly warm climate in the low latitude during the Eocene. An overall decreasing trend of the pCO_2 level was presented after the middle Eocene (Fig. 6; Retallack, 2009b). The ice-sheets started to appear in the Antarctic during the Late Eocene (Zachos et al., 2001), then the temperature suffered an apparent further decrease from the late Eocene onwards (Fig. 6).

In conclusion, although various results were made by different pCO_2 reconstruction proxies at the same time, their entire decreasing tendency of pCO_2 level is remarkably consistent with each other since the Eocene (Fig. 6). Figure 6 shows that during the Eocene the temperature was higher than at present. Comparing to the estimates of late middle Eocene pCO_2 by Doria et al. (2011), the present result of 351.9 ± 6.6 ppmv based on the regression approach shows a remarkably lower pCO_2 level, while the one based on the stomatal ratio method of 537.5 ± 56.5 ppmv is within the variation range of 500–1000 ppmv, which is closely consistent with the pCO_2 changes over the geological ages (Fig. 6). The world was dynamic in the Paleogene, including in the late middle Eocene, when the MECO occurred. Thus, the exact age matters, and it is possible that the values may differ because of slight offsets in time.

6 Conclusion

In this study, we reconstructed late middle Eocene pCO_2 based on the fossil leaves of *Nageia maomingensis* Jin et Liu from late middle Eocene of Maoming Basin, Guangdong Province, China. *Nageia* is a special element in conifers by its broad multi-veined leaf that lacks mid-vein. The stomatal data analysis suggests that only stomatal densities (SD) from both sides of *Nageia motleyi* leaves have significant negative correlations with the atmospheric CO_2 concentration. The SD from the adaxial side gives the best correlation to the CO_2. Based on SDs, the pCO_2 concentration is reconstructed using both the regression approach and the stomatal ratio method. The pCO_2 result based on the regression approach is 351.9 ± 6.6 ppmv, showing a relatively lower CO_2 level. The reconstructed result based on the stomatal ratio method is 537.5 ± 56.5 ppmv, consistent with the variation trends based on the other proxies. Here, we explored the potential of *N. maomingensis* in pCO_2 reconstruction and obtained different results according to different methods, providing a new insight for the reconstruction of paleoclimate and paleoenvironment in conifers.

Acknowledgements. This study was supported by the National Natural Science Foundation of China (Grant Nos. 41210001, 41572011), the Fundamental Research Funds for the Central Universities, and the Scientific Research Fund, Hongda Zhang, Sun Yat-sen University. We greatly thank the Herbarium of the V. L. Komarov Botanical Institute of the Russian Academy of Sciences (LE) for the permission to examine and collect extant *Nageia* specimens. We also express sincere gratitude to Sun Tongxing (Yancheng Teachers University), David Boufford (Harvard University) and Richard Chung Cheng Kong (Forest Research Institute Malaysia) for providing extant *N. motleyi* leaves from the herbarium of the Royal Botanic Garden at Edinburgh (E), the Harvard University Herbaria (A/GH) and the herbarium of Forest Research Institute Malaysia (KEP). We sincerely appreciate the guidance of Chengqian Wang (Harbin Institute of Technology) on preparing Figs. 3–6. We also offer sincere gratitude to Steven R. Manchester and Terry Lott (Florida Museum of Natural History, University of Florida) for suggestions and modification.

Edited by: G. Dickens

References

Bai, Y. J., Chen, L. Q., Ranhotra, S. P., Wang, Q., Wang, Y. F., and Li, C. S.: Reconstructing atmospheric CO_2 during the Plio–Pleistocene transition by fossil *Typha*, Glob. Change Biol., 21, 874–881, doi:10.1111/gcb.12670, 2015.

Beerling, D. J.: Stomatal density and index: theory and application, in: Fossil Plants and Spores: Modern Techniques, edited by: Jones, T. P. and Rowe, N. P., Geological Society, London, 251–256, 1999.

Beerling, D. J., and Kelly, C. K.: Stomatal density responses of temperate woodland plants over the past seven decades of CO_2 increase: A comparison of salisbury (1927) with contemporary data, Am. J. Bot., 84, 1572–1583, 1997.

Beerling, D. J. and Royer, D. L.: Reading a CO_2 signal from fossil stomata, New Phytol., 153, 387–397, doi:10.1046/j.0028-646X.2001.00335.x, 2002.

Beerling, D. J. and Royer, D. L.: Convergent Cenozoic CO_2 history, Nat. Geosci., 4, 418–420, doi:10.1038/ngeo1186, 2011.

Beerling, D. J., Chaloner, W. G., Huntley, B., Pearson, J. A., Tooley, M. J., and Woodward, F. I.: Variations in the stomatal density of *Salix herbacea* L. under the changing atmospheric CO_2 concentrations of late- and post-glacial time, Philos. T. R. Soc. Lon. B, 336, 215–224, doi:10.1098/rstb.1992.0057, 1992.

Beerling, D. J., Lomax, B. H., Royer, D. L., Upchurch Jr., G. R., and Kump, L. R.: An atmospheric pCO_2 reconstruction across the Cretaceous-Tertiary boundary from leaf megafossils, P. Natl. Acad. Sci. USA, 99, 7836–7840, doi:10.1073/pnas.122573099, 2002.

Beerling, D. J., Fox, A., and Anderson, C. W.: Quantitative uncertainty analyses of ancient atmospheric CO_2 estimates from fossil leaves, Am. J. Sci., 309, 775–787, doi:10.2475/09.2009.01, 2009.

Berner, R. A.: GEOCARB II: A revised model of atmospheric CO_2 over Phanerozoic time, Am. J. Sci., 294, 56–91, doi:10.2475/ajs.294.1.56, 1994.

Berner, R. A. and Kothavalá, Z.: GEOCARB III: A revised model of atmospheric CO_2 over Phanerozoic time, Am. J. Sci., 301, 182–204, doi:10.2475/ajs.301.2.182, 2001.

Bijl, P. K., Houben, A. J. P., Schouten, S., Bohaty, S. M., Sluijs, A., Reichart, G., Sinninghe Damsté, J. S., and Brinkhuis, H.: Transient middle Eocene atmospheric CO_2 and temperature variations, Science, 330, 819–821, doi:10.1126/science.1193654, 2010.

Brown, L. R.: Atmospheric carbon dioxide concentration, 1000–2009 (Supporting data), in: World on the Edge: How to Prevent Environmental and Economic Collapse, Chapter 4 Data: Rising Temperatures, Melting Ice, and Food Security, edited by: Brown, L. R., Earth Policy Institute, Norton, W. W. and Company, New York, London, available at: http://www.earth-policy.org/books/wote/wote_data, last access: 25 January 2016, 2010.

Cerling, T. E.: Use of carbon isotopes in paleosols as an indicator of the $P(CO_2)$ of the paleoatmosphere, Global Biogeochem. Cy., 6, 307–314, doi:10.1029/92GB01102, 1992.

Chaloner, W. G. and McElwain, J. C.: The fossil plant record and global climate change, Rev. Palaeobot. Palyno., 95, 73–82, doi:10.1016/S0034-6667(96)00028-0, 1997.

Cheng, W. C., Fu, L. K., and Chao, C. S.: *Podocarpus* (Podocarpaceae), in: Flora of China, edited by: Cheng, W. and Fu, L., Science Press, Beijing, 7, 398–422, 1978 (in Chinese).

Doria, G., Royer, D. L., Wolfe, A. P., Fox, A., Westgate, J. A., and Beerling, D. J.: Declining atmospheric CO_2 during the late Middle Eocene climate transition, Am. J. Sci., 311, 63–75, doi:10.2475/01.2011.03, 2011.

Ekart, D. D., Cerling, T. E., Montanez, I. P., and Tabor, N. J.: A 400 million year carbon isotope record of pedogenic carbonate: implications for paleoatmospheric carbon dioxide, Am. J. Sci., 299, 805–827, doi:10.2475/ajs.299.10.805, 1999.

Fletcher, B. J., Brentnall, S. J., Anderson, C. W., Berner, R. A., and Beerling, D. J.: Atmospheric carbon dioxide linked with Mesozoic and early Cenozoic climate change, Nat. Geosci., 1, 43–48, doi:10.1038/ngeo.2007.29, 2008.

Freeman, K. H. and Hayes, J. M.: Fractionation of carbon isotopes by phytoplankton and estimates of ancient CO_2 levels, Global Biogeochem. Cy., 6, 185–198, doi:10.1029/92GB00190, 1992.

Fu, D. Z.: Nageiaceae – a new gymnosperm family, Acta Phytotaxon. Sin., 30, 515–528, 1992 (in Chinese with English summary).

Fu, L. K., Li, Y., and Mill, R. R.: Podocarpaceae, in: Flora of China, edited by: Wu, Z. Y. and Raven, P. H., Science Press, Beijing, 4, 78–84, 1999.

Gale, J.: Availability of carbon dioxide for photosynthesis at high altitudes: theoretical considerations, Ecology, 53, 494–497, doi:10.2307/1934239, 1972.

Greenwood, D. G., Scarr, M. J., and Christophel, D. C.: Leaf stomatal frequency in the Australian tropical rain forest tree *Neolitsea dealbata* (Lauraceae) as a proxy measure of atmospheric pCO_2, Palaeogeogr. Palaeocl., 196, 375–393, doi:10.1016/S0031-0182(03)00465-6, 2003.

Grein, M., Oehm, C., Konrad, W., Utescher, T., Kunzmann, L., and Roth-Nebelsick, A.: Atmospheric CO_2 from the late Oligocene to early Miocene based on photosynthesis data and fossil leaf characteristics, Palaeogeogr. Palaeocl., 374, 41–51, doi:10.1016/j.palaeo.2012.12.025, 2013.

Henderiks, J. and Pagani, M.: Coccolithophore cell size and the Paleogene decline in atmospheric CO_2, Earth Planet. Sc. Lett., 269, 575–583, doi:10.1016/j.epsl.2008.03.016, 2008.

Hill, R. S. and Pole, M. S.: Leaf and shoot morphology of extant *Afrocarpus*, *Nageia* and *Retrophyllum* (Podocarpaceae) species, and species with similar leaf arrangement, from Tertiary sediments in Australasia, Aust. Syst. Bot., 5, 337–358, doi:10.1071/SB9920337, 1992.

Hu, J. J., Xing, Y. W., Turkington, R., Jacques, F. M. B. Su, T., Huang, Y. J., and Zhou, Z. K.: A new positive relationship between pCO_2 and stomatal frequency in *Quercus guyavifolia* (Fagaceae): a potential proxy for palaeo-CO_2 levels, Ann. Bot.-London, 115, 777–788, doi:10.1093/aob/mcv007, 2015.

Huang, C. M., Retallack, G. J., Wang, C. S., and Huang, Q. H.: Paleoatmospheric pCO_2 fluctuations across the Cretaceous-Tertiary boundary recorded from paleosol carbonates in NE China, Palaeogeogr. Palaeocl., 385, 95–105, doi:10.1016/j.palaeo.2013.01.005, 2013.

Jacques, F. M. B., Shi, G. L., Li, H. M., and Wang, W. M.: An early-middle Eocene Antarctic summer monsoon: Evidence of "fossil climates", Gondwana Res., 25, 1422–1428, doi:10.1016/j.gr.2012.08.007, 2014.

Jin, J. H., Qiu, J., Zhu, Y. A., and Kodrul, T. M.: First fossil record of the genus *Nageia* (Podocarpaceae) in South China and its phytogeographic implications, Plant Syst. Evol., 285, 159–163, doi:10.1007/s00606-010-0267-4, 2010.

Jones, H. G.: Plants and Microclimate, Cambridge University Press, Cambridge, UK, 1–428, 1992.

Kato, Y., Fujinaga, K., and Suzuki, K.: Marine Os isotopic fluctuations in the early Eocene greenhouse interval as recorded by metalliferous umbers from a Tertiary ophiolite in Japan, Gondwana Res., 20, 594–607, doi:10.1016/j.gr.2010.12.007, 2011.

Keating-Bitonti, C. R., Ivany, L. C., Affek, H. P., Douglas, P., and Samson, S. D.: Warm, not super-hot, temperatures in the early Eocene subtropics, Geology, 39, 771–774, doi:10.1130/G32054.1, 2011.

Kimura, T., Ohana, T., and Mimoto, K.: Discovery of a podocarpaceous plant from the Lower Cretaceous of Kochi Prefecture, in the outer zone of southwest Japan, P. Jpn. Acad. B-Phys., 64, 213–216, doi:10.2183/pjab.64.213, 1988.

Koch, P. L., Zachos, J. C., and Gingerich, P. D.: Correlation between isotope records in marine and continental carbon reservoirs near the Palaeocene/Eocene boundary, Nature, 358, 319–322, doi:10.1038/358319a0, 1992.

Kouwenberg, L. L. R., McElwain, J. C., Kürschner, W. M., Wagner, F., Beerling, S. J., Mayle, F. E., and Visscher, H.: Stomatal frequency adjustment of four conifer species to historical changes in atmospheric CO_2, Am. J. Bot., 90, 610–619, 2003.

Körner, Ch. and Cochrane, P. M.: Stomatal responses and water relations of *Eucalyptus pauciflora* in summer along an elevational gradient, Oecologia, 66, 443–455, doi:10.1007/BF00378313, 1985.

Krassilov, V. A.: New coniferales from Lower Cretaceous of Primorye, Bot. J., 50, 1450–1455, 1965 (in Russian).

Kürschner, W. M., van der Burgh, J., Visscher, H., and Dilcher, D. L.: Oak leaves as biosensors of late Neogene and early Pleistocene paleoatmospheric CO_2 concentrations, Mar. Micropaleontol., 27, 299–312, doi:10.1016/0377-8398(95)00067-4, 1996.

Kürschner, W. M., Wagner, F., Dilcher, D. L., and Visscher, H.: Using fossil leaves for the reconstruction of Cenozoic paleoatmospheric CO_2 concentrations, in: Geological Perspectives of Global Climate Change, edited by: Gerhard, L. C., Harrison, W. E., and Hanson, B. M., APPG Studies in Geology, 47, Tulsa, 169–189, 2001.

Kürschner, W. M., Kvaček, Z., and Dilcher, D. L.: The impact of Miocene atmospheric carbon dioxide fluctuations on climate and

the evolution of terrestrial ecosystems, P. Natl. Acad. Sci. USA, 105, 449–453, doi:10.1073/pnas.0708588105, 2008.

Liu, X. Y., Gao, Q., and Jin, J. H.: late Eocene leaves of *Nageia* Gaertner (section *Dammaroideae* Mill) from Maoming Basin, South China and their implications on phytogeography, J. Syst. Evol., 999, 1–11, doi:10.1111/jse.12133, 2015.

Lowenstein, T. K. and Demicco, R. V.: Elevated Eocene atmospheric CO_2 and its subsequent decline, Science, 313, 1928, doi:10.1126/science.1129555, 2006.

Maxbauer, D. P., Royer, D. L., and LePage, B. A.: High Artic forests during the middle Eocene supported by moderate levels of atmospheric CO_2, Geology, 42, 1027–1030, doi:10.1130/G36014.1, 2014.

McElwain, J. C.: Do fossil plants signal palaeoatmospheric carbon dioxide concentration in the geological past?, Philos. T. R. Soc. Lon. B, 353, 83–96, doi:10.1098/rstb.1998.0193, 1998.

McElwain, J. C. and Chaloner, W. G.: Stomatal density and index of fossil plants track atmospheric carbon dioxide in the Palaeozoic, Ann. Bot.-London, 76, 389–395, doi:10.1006/anbo.1995.1112, 1995.

McElwain, J. C. and Chaloner, W. G.: The fossil cuticle as a skeletal record of environmental changes, Palaios, 11, 376–388, doi:10.2307/3515247, 1996.

Mill, R. R.: A new combination in *Nageia* (Podocarpaceae), Novon, 9, 77–78, 1999.

Mill, R. R.: A new sectional combination in *Nageia* Gaertn. (Podocarpaceae), Edinburgh J. Bot., 58, 499–501, doi:10.1017/S0960428601000804, 2001.

Moran, K., Backman, J., Brinkhuis, H., Clemens, S. C., Cronin, T., Dickens, G. R., Eynaud, F., Gattacceca, J., Jakobsson, M., Jordan, R. W., Kaminski, M., King, J., Koc, N., Krylov, A., Martinez, N., Matthiessen, J., McInroy, D., Moore, T. C., Onodera, J., O'Regan, M., Pälike, H., Rea, B., Rio, D., Sakamoto, T., Smith, D. C., Stein, R., St John, K., Suto, I., Suzuki, N., Takahashi, K., Watanabe, M., Yamamoto, M., Farrell, J., Frank, M., Kubik, P., Jokat, W., and Kristoffersen, Y.: The Cenozoic palaeoenvironment of the Arctic Ocean, Nature, 441, 601–605, doi:10.1038/nature04800, 2006.

Nordt, L., Atchley, S., and Dworkin, S. I.: Paleosol barometer indicates extreme fluctuations in atmospheric CO_2 across the Cretaceous-Tertiary boundary, Geology, 30, 703–706, doi:10.1130/0091-7613(2002)030<0703:PBIEFI>2.0.CO;2, 2002.

Pagani, M., Arthur, M. A., and Freeman, K. H.: Miocene evolution of atmospheric carbon dioxide, Paleoceanography, 14, 273–292, doi:10.1029/1999PA900006, 1999.

Pagani, M., Zachos, J. C., Freeman, K. H., Tipple, B., and Bohaty, S.: Marked decline in atmospheric carbon dioxide concentrations during the Paleocene, Science, 309, 600–603, doi:10.1126/science.1110063, 2005.

Pearson, P. N., Foster, G. L., and Wade, B. S.: Atmospheric carbon dioxide through the Eocene-Oligocene climate transition, Nature, 461, 1110–1113, doi:10.1038/nature08447, 2009.

Petit, J. R., Jouzel, J., Raynaud, D., Barkov, N. I., Barnola, J.-M., Basile, I., Bender, M., Chappellaz, J., Davis, M., Delaygue, G., Delmotte, M., Kotlyakov, V. M., Legrand, M., Lipenkov, V. Y., Lorius, C., PÉpin, L., Ritz, C., Saltzman, E., and Stievenard, M.: Climate and atmospheric history of the past 420,000 years from the Vostokicecore, Antarctica, Nature, 399, 429–436, doi:10.1038/20859, 1999.

Pieter, T. and Keeling, R.: Recent monthly average Mauna Loa CO_2, NOAA/ESRL, available at: www.esrl.noaa.gov/gmd/ccgg/trends/ (last access: March 2015), 2015.

Poole, I. and Kürschner, W. M.: Stomatal density and index: the practice, in: Fossil Plants and Spores: Modern Techniques, edited by: Jones, T. P. and Rowe, N. P., Geological Society, London, 257–260, 1999.

Retallack, G. J.: A 300-million-year record of atmospheric carbon dioxide from fossil plant cuticles, Nature, 411, 287–290, doi:10.1038/35077041, 2001.

Retallack, G. J.: Greenhouse crises of the past 300 million years, Geol. Soc. Am. Bull., 121, 1441–1455, doi:10.1130/B26341.1, 2009a.

Retallack, G. J.: Refining a pedogenic-carbonate CO_2 paleobarometer to quantify a middle Miocene greenhouse spike, Palaeogeogr. Palaeocl., 281, 57–65, doi:10.1016/j.palaeo.2009.07.011, 2009b.

Roth-Nebelsick, A., Grein, M., Utescher, T., and Konrad, W.: Stomatal pore length change in leaves of Eotrigonobalanus furcinervis (Fagaceae) from the Late Eocene to the Latest Oligocene and its impact on gas exchange and CO_2 reconstruction, Rev. Palaeobot. Palyno., 174, 106–112, doi:10.1016/j.revpalbo.2012.01.001, 2012.

Roth-Nebelsick, A., Oehm, C., Grein, M., Utescher, T., Kunzmann, L., Friedrich, J.-P., and Konrad, W.: Stomatal density and index data of Platanus neptuni leaf fossils and their evaluation as a CO_2 proxy for the Oligocene, Rev. Palaeobot. Palyno., 206, 1–9, doi:10.1016/j.revpalbo.2014.03.001, 2014.

Royer, D. L.: Stomatal density and stomatal index as indicators of paleoatmospheric CO_2 concentration, Rev. Palaeobot. Palyno., 114, 1–28, doi:10.1016/S0034-6667(00)00074-9, 2001.

Royer, D. L.: Estimating latest Cretaceous and Tertiary atmospheric CO_2 from stomatal indices, in: Causes and Consequences of Globally Warm Climates in the early Paleocene, edited by: Wing, S. L., Gingerich, P. D., Schmitz, B., and Thomas, E., Geological Society of America Special Paper, 79–93, 2003.

Royer, D. L.: CO_2-forced climate thresholds during the Phanerozoic, Geochim. Cosmochim. Ac., 70, 5665–5675, doi:10.1016/j.gca.2005.11.031, 2006.

Royer, D. L., Wing, S. L., Beerling, D. J., Jolley, D. W., Koch, P. L., Hickey, L. J., and Berner, R. A.: Paleobotanical evidence for near present-day levels of atmospheric CO_2 during part of the Tertiary, Science, 292, 2310–2313, doi:10.1126/science.292.5525.2310, 2001.

Rundgren, M. and Beerling, D. J.: A Holocene CO_2 record from the stomatal index of subfossil *Salix herbacea* L. leaves from northern Sweden, Holocene, 9, 509–513, doi:10.1191/095968399677717287, 1999.

Seki, O, Foster, G. L., Schmidt, D. N., Mackensen, A., Kawamura, K., and Pancost, R. D.: Alkenone and boron-based Pliocene pCO_2 records, Earth Planet. Sc. Lett., 292, 201–211, doi:10.1016/j.epsl.2010.01.037, 2010.

Sinha, A. and Stott, L. D.: New atmospheric pCO_2 estimates from paleosols during the late Paleocene/early Eocene global warming interval, Global Planet. Change, 9, 297–307, doi:10.1016/0921-8181(94)00010-7, 1994,

Smith, R. Y., Greenwood, D. R., and Basinger, J. F.: Estimating paleoatmospheric pCO_2 during the early Eocene Climatic Optimum from stomatal frequency of *Ginkgo*, Okanagan Highlands, British Columbia, Canada, Palaeogeogr. Palaeocl., 293, 120–131, doi:10.1016/j.palaeo.2010.05.006, 2010.

Spicer, A. R., Herman, A. B., Liao, W. B., Spicer, T. E. V., Kodrul, T. M., Yang, J., and Jin, J. H.: Cool tropics in the middle Eocene: Evidence from the Changchang Flora, Hainan Island, China, Palaeogeogr. Palaeocl., 412, 1–16, doi:10.1016/j.palaeo.2014.07.011, 2014.

Stott, L. D.: Higher temperatures and lower oceanic pCO_2: A climate enigma at the end of the Paleocene Epoch, Paleoceanography, 7, 395–404, doi:10.1029/92PA01183, 1992.

Stults, D. Z., Wagner-Cremer, F., and Axsmith, B. J.: Atmospheric paleo-CO_2 estimates based on *Taxodium distichum* (Cupressaceae) fossils from the Miocene and Pliocene of Eastern North America, Palaeogeogr. Palaeocl., 309, 327–332, doi:10.1016/j.palaeo.2011.06.017, 2011.

Sun, B. N., Ding, S. T., Wu, J. Y., Dong, C., Xie, S. P., and Lin, Z. C.: Carbon isotope and stomatal data of late Pliocene Betulaceae leaves from SW China: Implications for palaeoatmospheric CO_2-levels, Turk. J. Earth Sci., 21, 237–250, doi:10.3906/yer-1003-42, 2012.

Sun, T. X.: Cuticle micromorphology of *Nageia*, J. Wuhan Bot. Res., 26, 554–560, doi:10.3969/j.issn.2095-0837.2008.06.002, 2008 (in Chinese with English abstract).

Tripati, A. K., Roberts, C. D., and Eagle, R. A.: Coupling of CO_2 and ice sheet stability over major climate transitions of the last 20 million years, Science, 326, 1394–1397, doi:10.1126/science.1178296, 2009.

Van der Burgh, J., Visscher, H., Dilcher, D. L., and Kürschner, W. M.: Paleoatmospheric signatures in Neogene fossil leaves, Science, 260, 1788–1790, doi:10.1126/science.260.5115.1788, 1993.

Walker, J. D. and Geissman, J. W.: Geologic Time Scale, Geological Society of America, doi:10.1130/2009.CTS004R2C, available at: http://www.geosociety.org/science/timescale/, last access: 25 January 2016, 2009.

Wang, J. D., Li, H. M., and Zhu, Z. Y.: Magnetostratigraphy of Tertiary rocks from Maoming Basin, Guangdong province, China, Chinese Journal of Geochemistry, 13, 165–175, doi:10.1007/BF02838516, 1994.

Wing, S. L., Harrington, G. J., Smith, F. A., Bloch, J. I., Boyer, D. M., and Freeman, K. H.: Transient floral change and rapid global warming at the Paleocene-Eocene boundary, Science, 310, 993–996, doi:10.1126/science.1116913, 2005.

Woodward, F. I.: Ecophysiological studies on the shrub *Vaccinium myrtillus* L. taken from a wide altitudinal range, Oecologia, 70, 580–586, doi:10.1007/BF00379908, 1986.

Woodward, F. I.: Stomatal numbers are sensitive to increases in CO_2 concentration from pre-industrial levels, Nature, 327, 617–618, doi:10.1038/327617a0, 1987.

Woodward, F. I. and Bazzaz, F. A.: The responses of stomatal density to CO_2 partial pressure, J. Exp. Bot., 39, 1771–1781, doi:10.1093/jxb/39.12.1771, 1988.

Yang, J. J., Qi, G. F., and Xu, R. H.: Studies on fossil woods excavated from the Dabie mountains, Sci. Silvae Sinicae, 26, 379–386, 1990 (in Chinese with English abstract).

Ye, M. N.: On the preparation methods of fossil cuticle, in: Selected papers of the 12th Annual conference of the Palaeontological Society of China, edited by: Palaeontological Society of China, Science Press, Beijing, 170–179, 1981 (in Chinese).

Zachos, J., Pagani, M., Sloan, L., Thomas, E., and Billups, K.: Trends, rhythms, aberrations in global climate 65 Ma to present, Science, 292, 686–693, doi:10.1126/science.1059412, 2001.

Zachos, J., Dickens, G. R., and Zeebe, R. E.: An early Cenozoic perspective on greenhouse warming and carbon-cycle dynamics, Nature, 451, 279–283, doi:10.1038/nature06588, 2008.